ISSN 0001-4370, Oceanology, 2017, Vol. 57, No. 1, pp. 165–173. © Pleiades Publishing, Inc., 2017.
Original Russian Text © V.V. Pelevin, P.O. Zavjalov, N.A. Belyaev, B.V. Konovalov, M.D. Kravchishina, S.A. Mosharov, 2017, published in Okeanologiya, 2017, Vol. 57, No. 1, pp. 183–193.

MARINE GEOLOGY

Spatial Variability of Concentrations of Chlorophyll *a*, Dissolved Organic Matter and Suspended Particles in the Surface Layer of the Kara Sea in September 2011 from Lidar Data

V. V. Pelevin*, P. O. Zavjalov, N. A. Belyaev, B. V. Konovalov, M. D. Kravchishina, and S. A. Mosharov

Shirshov Institute of Oceanology, Moscow, Russia

**e-mail: vvpelevin@gmail.com*

Received June 18, 2015; in final form, June 29, 2016

Abstract—The article presents results of underway remote laser sensing of the surface water layer in continuous automatic mode using the UFL-9 fluorescent lidar onboard the R/V *Akademik Mstislav Keldysh* during cruise 59 in the Kara Sea in 2011. The description of the lidar, the approach to interpreting seawater fluorescence data, and certain methodical aspects of instrument calibration and measurement are presented. Calibration of the lidar is based on laboratory analysis of water samples taken from the sea surface during the cruise. Spatial distribution of chlorophyll *a*, total organic carbon and suspended matter concentrations in the upper quasi-homogeneous layer are mapped and the characteristic scales of the variability are estimated. Some dependencies between the patchiness of the upper water layer and the atmospheric forcing and freshwater runoff are shown.

DOI: 10.1134/S0001437017010131

1. INTRODUCTION

Remote sensing of the sea surface layer with a shipborne fluorescence lidar makes it possible to obtain the real-time information on the spatial distributions of phytoplankton chlorophyll, CDOM, and total suspended matter [9, 12, 19–22].

As a rule, the highest content of terrigenous matter in the shelf waters of seas occurs in the upper thin layer of the most desalinated water, where continental runoff desalinates the surface layer and vertical density stratification is particularly strong. This is typical of the Kara Sea basin, influenced by intense continental runoff from the Ob and Yenisei rivers. The latter supply the Kara Sea Basin with large masses of mineral particles, substances of organic origin, and nutrients. The occurrence of well-defined and fairly narrow (from hundreds of meters to tens of centimeters) frontal zones, the large variety of meso- and submesoscale structures, and considerable distribution of river plumes throughout the sea surface is characteristic of the Kara Sea (see, e.g., [6]).

A lidar senses the sea through the air–water interface. Consequently, a surface film of any thickness contributes to the fluorescence signal [20]. This is beyond the scope of any express measurements based on underway water sampling from a fixed depth level. In addition, a lidar interacts with an undisturbed water medium in real time without any lags and smoothing of high-frequency fluctuations. As for other kinds of remote sensing techniques, a lidar has advantages as an active tool over passive ones. These are, e.g., shipborne or orbiting radiometers, that depend on illumination conditions and rank below lidars in sensitivity and accuracy. In spite of the synopticity and regularity of satellite radiometric observations, they are useless under cloudy conditions and miss fine structures of spatial distributions. This prevents the use of orbiting radiometers for studying submesoscale variability of the upper layer of seas, particularly at high latitudes. The UFL-9 fluorescence lidar provides comprehensive facilities for studying submesoscale (1–10 km) and small-scale (1–1000 m) phenomena in the upper sea layer owing to high spatial resolution, wide sensitivity range, and the ability to concurrently record three physical characteristics of seawater [1, 13, 35].

Over the past 30–40 years, the patchiness of oceanic properties were studied by means of instrumentation on moving carriers (ships, aircrafts, satellites) and the measurement results were used to calculate the spatial spectra of admixture concentrations and environmental characteristics [17, 24, 25]. Numerous studies describe the spatial variability of planktonic communities [7, 8, 23, 28] and most of them are dedicated to zooplankton distributions at scales larger than 1 km (see, e.g., [25]). It is believed that small-scale variability, or patchiness, is primarily inherent to zooplankton, while phytoplankton varies more likely within the submesoscale range [37]. However, there are observations of small-scale variability of the phytoplankton concentration in the surface layer of seas

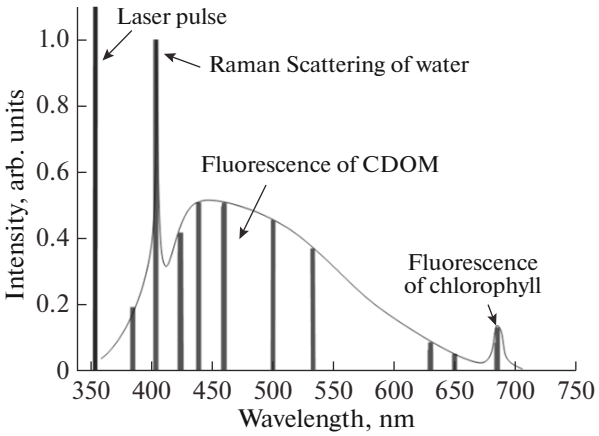

Fig. 1. Fluorescence spectrum of seawater and spectral channels of fluorescence lidar UFL-9.

and inland water basins [18], as well as microscale variability in the abundance of zooplankton [27]. Studies of the small-scale patchiness of organic [3, 33] and suspended matter [31, 32, 36] are scarce, apparently due to the lack of instruments for studies of this kind.

2. MATERIALS AND METHODS

Quasi-continuous remote sensing of the sea surface was carried out with a fluorescence lidar during cruise 59 of the R/V *Akademik Mstislav Keldysh*. The instrument was mounted on the bow 8.3 m above the sea surface. Lidars of the UFL series were developed at the Shirshov Institute of Oceanology, Russian Academy of Sciences (SIO RAS) in 2001–2009 and have successfully operated during 35 Institute expeditions in fresh, brackish, saline, and ultrasaline water basins. They are designed to measure the concentration of chlorophyll *a* (chl*a*), CDOM, and the total concentration of particles suspended in the sea water upper layer [1]. The thickness of the sensed layer, which we consider mixed, depends on water transparency and varies from a few tens of meters in the open ocean to tens of centimeters in turbid coastal waters loaded with mineral particles and organic compounds.

The chl *a* and CDOM contents are estimated based on analytical processing of fluorescence signals from the water medium. Signals of elastic backscattering of laser pulses from suspended particles are used to measure the suspended matter content. The initial intensities are normalized to Raman scattering of seawater [30, 35]. Figure 1 shows the spectrum of the incoming signal and spectral channels of the UFL-9 lidar. The measurements were performed in automatic mode at a rate of 2 Hz. The main specifications of the lidar are given in Table 1. The theory and techniques of UFL lidar measurements, based on laser-excited fluorescence and elastic backscattering in waters with widely varying trophicity, are given in [13, 14, 34, 35].

In addition, continuous underway sensing of the thermohaline state of the sea surface layer was conducted during the cruise with a flow-through CTD system. The water was sampled with a 1.5-kW Grundfos JP-6 upstream centrifugal pump through a 9-m flexible hose fed overboard from the operations deck. The input of the hose was fixed at a depth of about 1 m below the sea surface. The operational capacity of the pump was up to 0.8 L/s. Water was fed into a 70-L on-deck closed basin, in which the SeaBird SBE911 CTD probe was installed. Its data and GPS data were fed to a laboratory computer. The residence time of water in the basin was roughly 100 s, which yields a 500-m scale of data smoothing for a vessel speed of 10 knots.

Water sampling by bucket underway and at stations was carried out during the expedition, being time-referenced by lidar measurements. A large integral 50-L water sample was created for distribution among the analytical labs in order to ensure comparability of the results.

Table 1. Basic specifications of UFL-9UV fluorescent lidar

Excitation wavelength Receiving spectral channels	355, 532 nm 355, 385, 404, 424, 440, 460, 499, 532, 620, 651, 685 nm
Pulse frequency	2 Hz
Pulse length	6 ns
Pulse energy	1.5 mJ (355 nm), 3 mJ (532 nm)
Telescope system	Keplerian type, range to object adjustable from 1.5 to 25 m
Adjustable lens	140 mm
Power supply	220 V, 50 Hz, 120 W
Weight and size	35 Kg, 800 × 550 × 250 mm
Receivers	PMT, multialkaline cathode
Spectral selection	4-channel optical system, interference color filters
Sample rate ADC	50 MHz
ADC capacity	10 bit
Software	Windows XP, GPS positioning, on-line plotting of profile and data post-processing based on parameters required for plotting map of study area

Standard filtration in a 400 mbar vacuum was used to estimate the mass concentration (mg/L) of suspended matter retained by nuclear membrane filters (diameter 47 mm, pore diameter 0.45 μm). The concentration was found by weighing the filters with an accuracy of ±0.01 mg and the volume of filtered water. This technique is described in detail in [11].

A Shimadzu TOC-Vcph analyzer with an SSM-5000A attachment was used to determine suspended and dissolved organic carbon according to procedures explained in [2]. The same study reports the spatial distributions of organic carbon in the Kara Sea. The water samples were filtered through Whatman GF/F precalcinated filters with a rated pore diameter of 0.5-0.7 μm. The average volume of filtered water was ~10 L per station. The filtrate for determining dissolved organic carbon was acidified to pH = 2 and stored in a refrigerator. The frozen filter with sampled matter was stored at –20°C for later analysis.

GF/F fiberglass filters were used to determine chl *a* at an underpressure below 0.3 bar. Next, the filters were placed in 90% acetone and stored in the dark for 24 h at +4°C. The obtained extract was analyzed with a MEGA-25 fluorimeter, and the chl *a* content was calculated according to [15, 29]. In addition, the samples were analyzed at SIO RAS based on a standard spectrophotometric method [5]. For this purpose the samples were filtered through the fiberglass filters GF/F immediately after the sampling, dried out and frozen for consequent transportation. Depending on turbidity, the volume of filtered water varied from 5 to 8.25 L. Analysis of particles, retained by filters, and calculation of total concentrations of mineral and organic fractions was fulfilled according to techniques in [10].

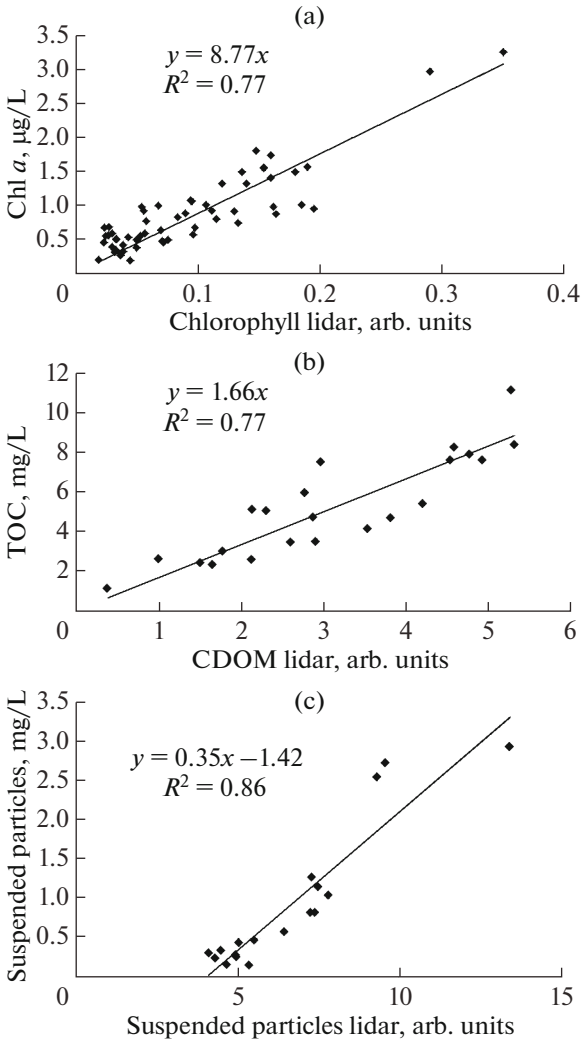

Fig. 2. Calibration of lidar from laboratory measurements of chl *a* (a), TOC (b), and mass content of particles (c) in water samples.

3. CALIBRATION OF LIDAR MEASUREMENTS

The lidar measurements need to be verified for every aquatic area and season of observations when they are used to map the spatial distribution in units of weight concentration. The lidar fluorescence and backscattering signals depend on the contents of specific substances in water and a multitude of other factors. In the case of chlorophyll fluorescence, these are the species composition of phytoplankton, the phase of succession and physiological state of the latter, and the conditions of the abiotic environment. The molecular composition of CDOM affects is fluorescence. Size distribution and chemical composition of mineral particles influence the backscattering signal.

We used the results of standard laboratory measurements of chl *a* (μg/L), the total organic carbon (TOC) (mg/L) as a sum of its suspended and dissolved fractions, and the mass concentration of suspended matter (mg/L). The obtained regressions are shown in Fig. 2. It should be noted that the fluorescence signal at 440 nm, close to the spectral maximum of CDOM fluorescence, was calibrated by TOC determinations as the most comprehensive and representative among organic matter determinations performed during expedition. Any organic matter, be it suspended or dissolved one, emits fluorescence excited by a laser pulse. That is why the TOC is the most convenient matter for finding correlation with the fluorescence signal.

We obtained coefficients of determination (R^2) for chl *a*, TOC, and suspended matter as high as 0.77, 0.77, and 0.86 respectively. The relatively moderate correlation of the lidar CDOM fluorescence and TOC from water sampling is attributable to the fact that laser light is absorbed by the colored fraction of organic matter occurring in the upper mixed layer (UML). The cruise route crossed coastal and offshore waters influenced by continental runoff waters of different origin. The latter carry organic matter of diverse molecular composition, which occurs as dissolved,

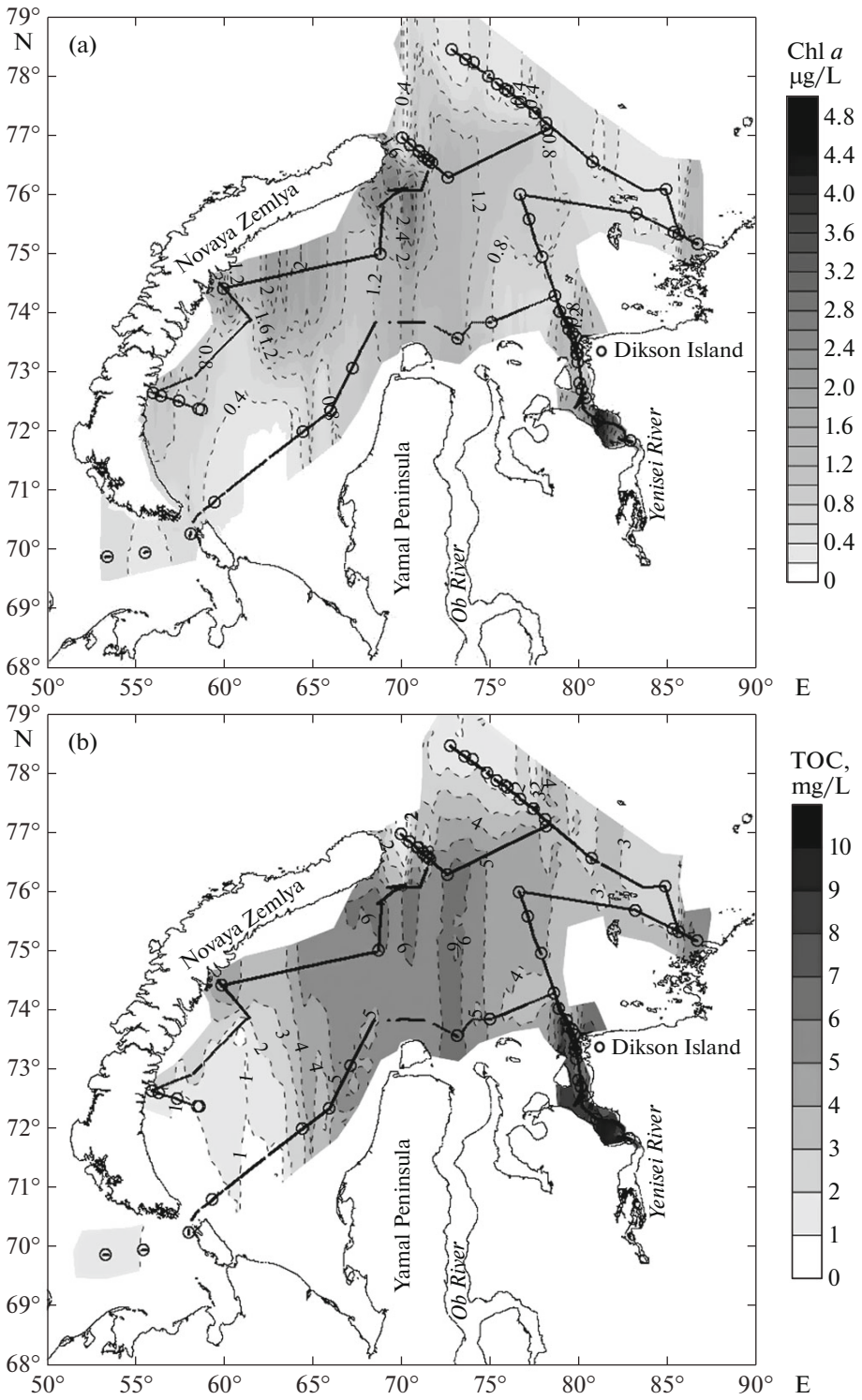

Fig. 3. Spatial distributions of chl*a* (a), TOC (b), and content of particles (c) along route of cruise 59 of R/V *Akademik Mstislav Keldysh*, 2011. Solid line designates route and circles mark sites of water sampling for lidar calibration.

colloidal, and suspended fractions [4, 32]. Strictly speaking, different components of organic matter contribute in various ways the lidar's fluorescence signal. The same mechanisms resulted in inconstancy of species composition of the phytoplankton lengthwise along the route [6]. The correlation of the lidar data and suspended matter content from water sampling is higher than in the case of the concentration dependence of fluorescence. Based on our experience, this is characteristic of other salt- and freshwater basins and

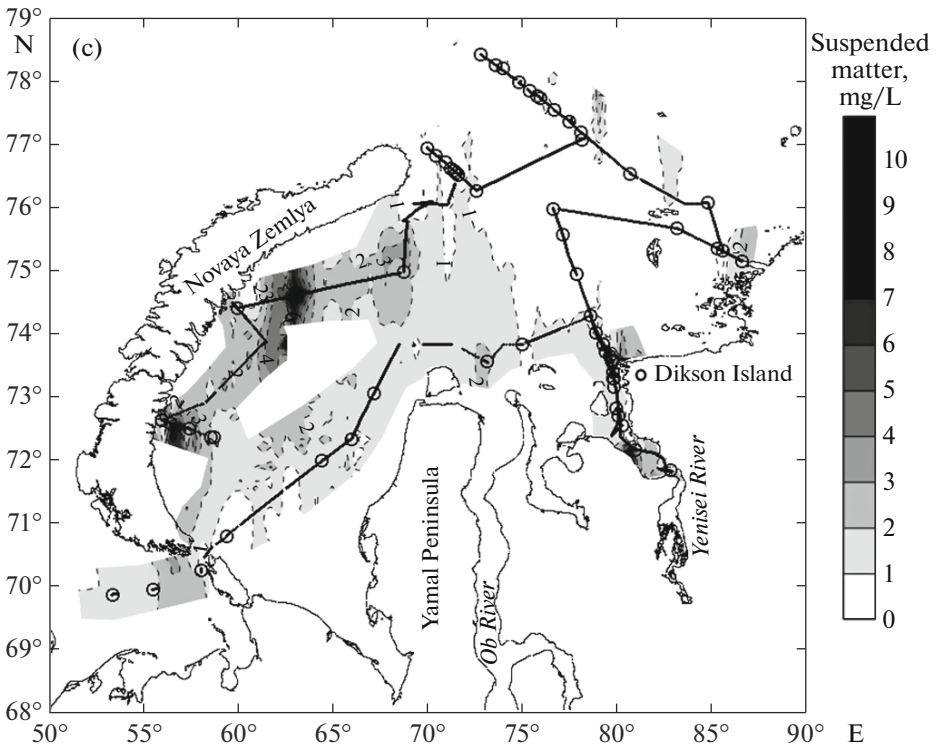

Fig. 3. (Contd.)

is due to the simpler mechanism by which the elastic backscattering signal forms from laser pulse compared to the fluorescence signal. By and large, with regard to the extent of the study area and duration of the expedition, the correlation of lidar signals and water sampling data is satisfactory.

4. SPATIAL VARIABILITY OF BIO-OPTICAL FIELDS OF THE KARA SEA

The submesoscale and microscale variability of chlorophyll, CDOM, and suspended matter within tens of meters to few kilometers is, apparently, the less understood phenomenon due to the lack of instrumental techniques for obtaining information of this kind. The satellite observations are inadequate in spatial resolution and it is difficult to perform high rate measurements using submersible instrumentation.

Continuous measurements were the only mode of lidar observations in the Kara Sea. Their results have been used to plot the spatial distributions of bio-optical characteristics corresponding to different scales, the whole sea area inclusive (Fig. 3). As a rule, the measured concentrations almost always increase in the surface layer of the Kara Sea under the impact of river runoff and the highest concentrations gravitate to river mouths or their plumes. The limits of variations of concentrations over the study area were 0.1–5 μg/L for chl *a*, 0.5–11 mg/L for TOC, and 0.1–5 mg/L for suspended matter with averaging of concentrations according to the spatial resolution of figures. However, the range of concentrations is much broader when dealing with small spatial scales (see Table 2 and comments below).

In this paper, our main concern is the variability on scales from tens of meters to kilometers. We assume a patchiness of distributions of phytoplankton, organic matter, and suspended particles in the absence of anisotropic distributions, such as surface filaments. This assumption agrees well with the published evi-

Table 2. Distribution of scales of patches over vessel itinerary. Total number of measurements of any parameter exceeds 600000. Concentrations of chl*a*, TOC, and suspended particles are given in μg/L, mg/L, and mg/L, respectively

	Mean scale, m	S_r, %	Minimum concentration	Maximum concentration	Maximum/ Minimum	Total number of patches
chl*a*	72	96	0.06	9	150	136743
TOC	24	53	0.25	20	80	134821
Susp. matter	46	150	1	33	33	131800

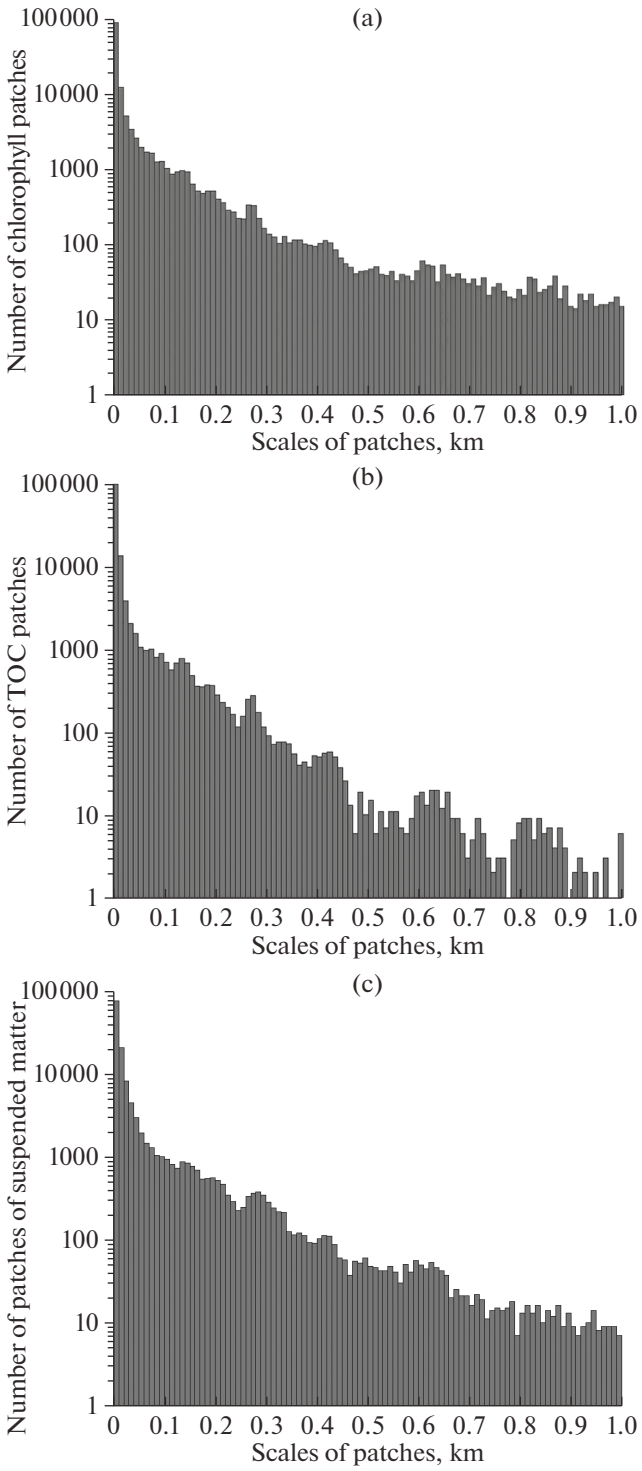

Fig. 4. Histograms of small scales of patches (up to 1 km for a step of 10 m) for chl *a* (a), TOC (b), and suspended particles (c) for the whole itinerary of cruise in Kara Sea. Number of patches is given in logarithmic scale.

dence [17, 18, etc.] and our own experience of field observations using UFL fluorescence lidars of series on dozens of field missions in diverse aquatic areas. Below, we attempt to describe the characteristics and certain statistical peculiarities of patchy structures on the basis of lidar data at small spatial scales. Studies of this kind had not been carried out earlier in the Kara Sea due to lack of data with adequate spatial resolution.

The following criterion for defining a boundary of an individual "patch" at each measurement point has been suggested: the occurrence of the first encountered change in the corresponding concentration by one-tenth of the standard deviation or more, calculated from the entire data set along the path of the vessel. This criterion has been chosen from qualitative considerations, and the calculations have been performed for every member of a series of an individual parameter. The statistics of patchiness are given in Table 2. The latter shows the mean sizes of patches, along with the minimum, maximum and average concentrations lengthwise the vessel's route as well as relative standard deviation (S_r) for every concentration as ratio of standard deviation to average value of data series. Our criterion is $0.1\,S_r$.

The number of measurements of any concentration exceeds 600000 for the whole area of the Kara Sea. According to our definition of patches, their dimensions varied from 10 m to 10 km. Noteworthy is the considerable difference between extreme estimates of the concentration for an individual parameter (150-fold for chl *a*, 80-fold for TOC, and 33-fold for suspended particles). These estimates are not outliers, attributable to a particular type of errors, but represent a considerable set of measurement data related to near-mouth areas in the case of the upper limit of concentration or to offshore waters in the case of low concentrations. As noted above, this variability is missing in maps for the whole study area due to inevitable averaging. However, it is evident at smaller scales, and hundreds of lidar measurements confirm every inhomogeneity. It should be mentioned that reference field data from water samples for lidar calibration belong to a much narrower range of concentrations. For this reason, we can trust the lidar measurements results, expressed in absolute units and covering a much broader range, if it is possible to admit the linearity of calculated regressions within the latter. This is unlikely because of the well-known nonlinearity of the regression equation with a high concentration of organic matter [34], the effect of fluorescence saturation [16, 22], and other factors. However, our estimates point to the orders of magnitudes of the quantities involved and emphasize the importance of a more thorough investigation of small-scale patchiness in the UML.

Consideration of small-scale patches (10–1000 m) allowed us to establish in greater detail that the spatial distribution of phytoplankton, as well as organic and suspended matter, can be represented as a superposition of patches with a wide range of scales. Their distributions obey a power law (see Fig. 4), which agrees with the inferences in [18]. The histograms in Figs. 4 and 5 have been plotted from the whole set of patches in the Kara Sea (about 130000 patches for every

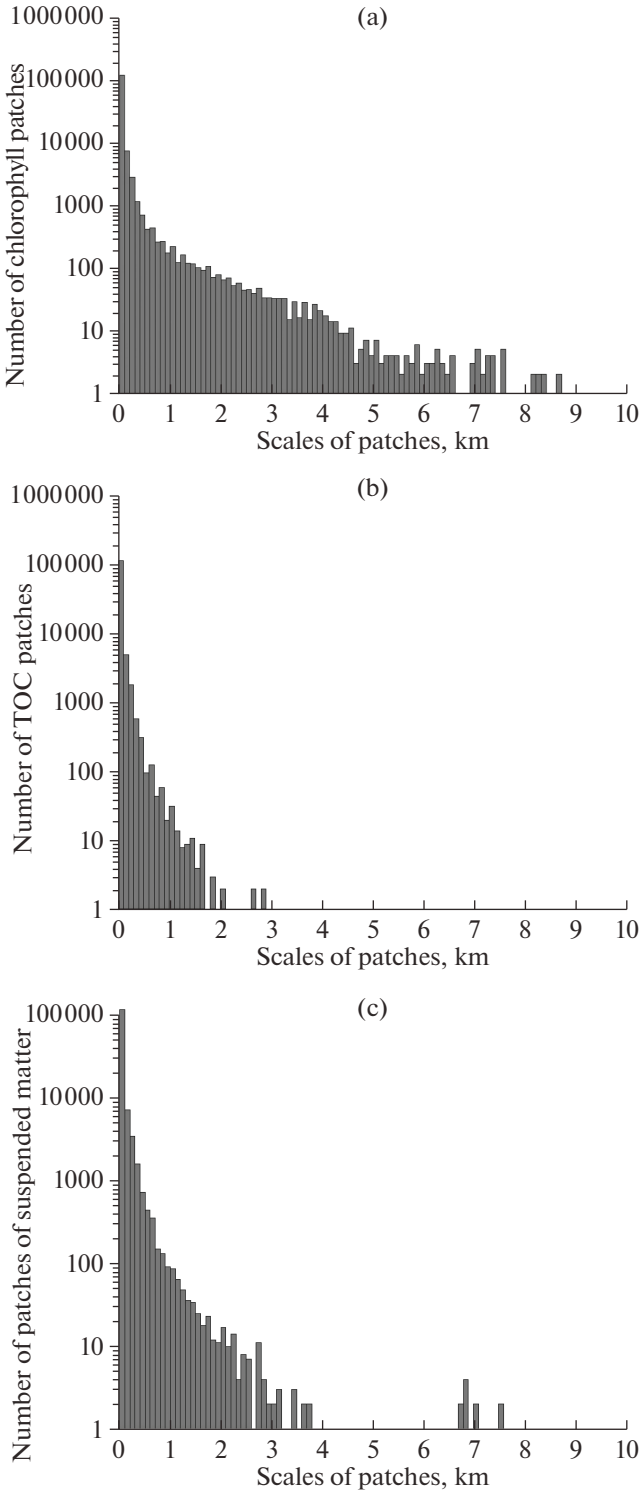

Fig. 5. Histograms of patches on scale up to 10 km (step of 100 m) for chl *a* (a), TOC (b), and suspended particles (c) for entire itinerary of cruise in Kara Sea. Number of patches is given in logarithmic scale.

parameter). In agreement with the power law of distribution of inhomogeneity scales, roughly 80% of patches belong to the subrange of scales smaller than the average.

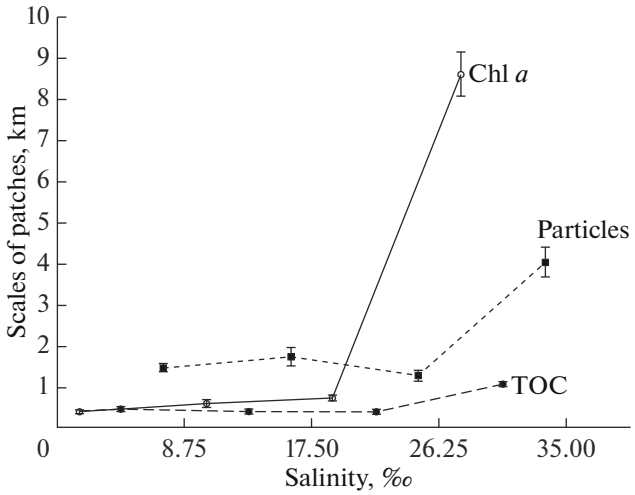

Fig. 6. Salinity dependence of scales of patches for chl *a*, TOC, and suspended particles (based on reduced selection of measurement data distributed evenly over the sea).

Figure 6 shows the relation of the patchiness scales of the studied parameters and salinity. This relation points to the occurrence of a certain dependence of the scale of patches on the distance to river mouths and desalinated waters, which agrees with earlier reported data [3]. The scales of inhomogeneities are smaller in active mixing areas, in the vicinity of river mouths, and other sources of continental runoff compared to offshore areas. As follows from analytical processing of the data from a 50-km transect inside Yenisei Bay south of Dikson Island, the structure of patchiness scales in waters with salinity below 18‰ differs from patterns found by averaging over the entire route of the vessel (Table 2). The minimum scales of patches of chlorophyll and organic matter and the maximum scales of patches of suspended particles are characteristic of the near-mouth zone.

Figure 7 shows the dependence of scales of patches on wind friction tension. Relatively larges scales of patches occur during gentle winds due to the lack of external forcing, which induce mixing of waters differing in temperature, salinity, and admixture content. Intensification of wind leads to a piecewise mixing, or stirring, which breaks up large patches and produces smaller ones. A description of this process and relevant mathematical modeling of this phenomenon is given in [18] with consideration for physical and biological factors of environment. Results of modeling give grounds to attribute small-scale natural inhomogeneities of phyto- and zooplankton to advective mixing of water masses in the surface layer. When interpreting Fig. 7, it is evident that further intensification of the wind leads to final mixing of individual small patches or various fragments. The scales of inhomogeneities continue to grow at stronger winds which finally results in homogeneity of surface layer of the sea. In general outline, this process corresponds to classical

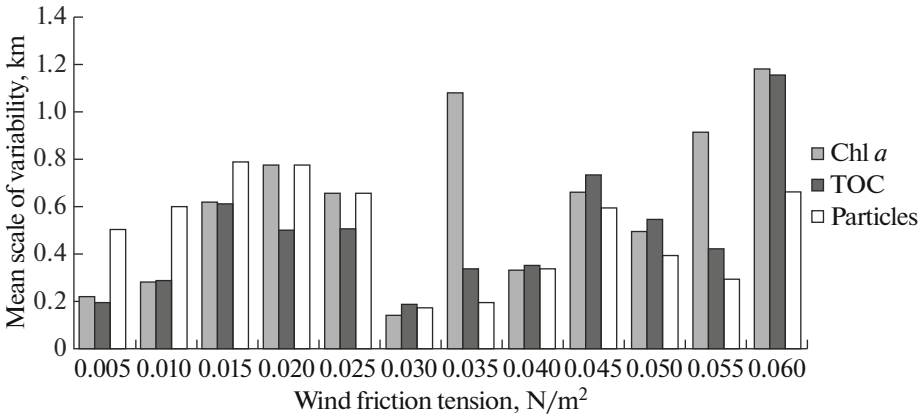

Fig. 7. Dependence of scales of patches of chl *a*, TOC, and suspended particles on wind friction tension (based on reduced selection of measurement data evenly distributed over the sea).

concept of stirring and mixing [26], but its manifestations in the Kara Sea were observed for the first time.

5. CONCLUSIONS

On board data collection with a fluorescence lidar with a fairly high pulse rate makes it possible to reveal fine structures in the variability of phytoplankton chlorophyll, organic matter, and suspended particles in the surface layer and to find the spatial distribution patterns of these parameters with a high spatial resolution. This reduces the need to sample large volumes of seawater, when it is necessary to obtain large volumes of data for a short period of time.

It is possible to map the distributions of chl *a*, organic matter (e.g. TOC), and mineral particles in units of concentrations when the lidar is calibrated from data of standard determinations of these quantities in water samples from the study area.

We have substantiated the idea of representing small-scale concentration inhomogeneities as a superposition of patches ranging in scales from 10 m to 10 km. The averaged patchiness scales obtained with the above processing of spatial series of concentrations of chl *a,* TOC, and suspended matter range from 24 to 72 m for different parameters and substantially depend on the oceanology of the study area. Among these patches, 80% belong to scales smaller than medium. When wind intensifies, the scales of patches initially decrease and then increase until homogeneity of the surface layer is reached. The scales increase with distance from sources of desalinated runoff and the coastal zone. Further studies are needed to clarify the reason for such a distribution of scales. The present work, dedicated to issues of patchiness of distributions of bio-optical fields, is a pilot project for the team of authors and will be continued on the basis of experience and materials obtained by high-rate lidar remote sensing.

ACKNOWLEDGMENTS

This study was supported by the Russian Science Foundation, project no. 14-17-00682 (determination of chlorophyll concentrations and data analysis). Expedition research was supported by the Russian Foundation for Basic Research (project no. 14-05-05003 Kar_a).

REFERENCES

1. N. A. Aibulatov, P. O. Zavialov, and V. V. Pelevin, "Specific hydrophysical self-purification of Russian coastal zone of the Black Sea near river estuaries," Geoekologiya, No. **4**, 301–310 (2008).
2. N. A. Belyaev, V. I. Peresypkin, and M. S. Ponyaev, "The organic carbon in the water, the particulate matter, and the upper layer of the bottom sediments of the west Kara Sea," Oceanology (Engl. Transl.) **50**, 706–715 (2010).
3. Yu. A. Goldin, A. V. Shatravin, V. A. Levchenko, Yu. I. Ventskut, B. A. Gureev, and O. V. Kopelevich, "Analysis of spatial variability of fluorescence intensity of the sea water in the western part of the Black Sea," Fundam. Prikl. Gidrofiz. **8** (1), 17–26 (2015).
4. V. V. Gordeev, *Geochemistry of the River-Sea System* (IP I.I. Matushkina, Moscow, 2012) [in Russian].
5. *GOST* (State Standard) *17.1.04.02-90: Water. Spectrophotometric Determination of Chlorophyll a* (State Committee on Environment Protection of Soviet Union, Moscow, 1990) [in Russian].
6. P. O. Zavialov, A. S. Izhitskiy, A. A. Osadchiev, V. V. Pelevin, and A. B. Grabovskiy, "The structure of thermohaline and bio-optical fields in the surface layer of the Kara Sea in September 2011," Oceanology (Engl. Transl.) **55**, 461–471 (2015).
7. V. V. Zavoruev, L. A. Levin, G. Ya. Rachenko, et al., "Spatio-temporal distribution of chlorophyll *a* in the water of Lake Baikal during winter," Gidrobiol. Zh. **28** (1), 17–24 (1992).
8. G. S. Karabashev, "Specific distribution pattern of fluorescence and light scattering at the intensive vertical mixing and water rise," Okeanologiya (Moscow) **17**, 312–318 (1977).

9. G. S. Karabashev, *Fluorescence in Ocean* (Gidrometeoizdat, Leningrad, 1987) [in Russian].
10. B. V. Konovalov, M. D. Kravchishina, N. A. Belyaev, et al., "Spectral analysis of marine suspended matter: alternative to traditional analysis methods used for ecological monitoring," *Proceedings of XII International Conference "Ecosystems, Organisms, and Innovations"* (Moscow State Univ., Moscow, 2010), Vol. 16, p. 17.
11. M. D. Kravchishina, A. Yu. Lein, I. N. Sukhanova, V. A. Artem'ev, and A. N. Novigatsky, "Genesis and spatial distribution of suspended particulate matter concentrations in the Kara Sea during maximum reduction of the Arctic ice sheet," Oceanology (Engl. Transl.) **55**, 623–643 (2015).
12. V. N. Pelevin, O. I. Abramov, and G. G. Carlsen, "Satellite ecological experiment in ten European seas," Inzh. Ekol., No. 6, 31–41 (1995).
13. V. N. Pelevin, O. I. Abramov, G. G. Carlsen, et al., "Laser survey of the surface waters of Atlantic and European sea," Opt. Atmos. Okeana **14**, 704–709 (2001).
14. V. N. Pelevin and V. A. Rutkovskaya, "Classification of ocean waters by spectral decay of the solar light," Okeanologiya (Moscow) **17**, 50–54 (1977).
15. S. I. Pogosyan, S. V. Gal'chuk, and Yu. V. Kizimirko, "Use of MEGA-25 fluorimeter for analysis of phytoplankton quantity and its photosynthetic apparatus," Voda: Khim. Ekol., No. 6, 34–40 (2009).
16. V. V. Fadeev, N. N. Sysoev, I. V. Fadeeva, S. A. Dolenko, and T. A. Dolenko, "On the potentiality of using the fluorescence of humic substances for the determination of hydrological structures in coastal sea waters and in inland water basins," Oceanology (Engl. Transl.) **52**, 566–575 (2012).
17. K. N. Fedorov and N. P. Kuz'mina, "Ocean fronts," in *Mesoscale Fluctuation of the Temperature Field in Ocean* (Institute of Oceanology, Academy of Sciences of Soviet Union, Moscow, 1977), pp. 33–53.
18. E. R. Abraham, "The generation of plankton patchiness by turbulent stirring," Nature **391**, 577–580 (1998).
19. O. I. Abramov, V. I. Eremin, G. G. Karlsen, et al., "Application of laser ranging to determine the pollution of sea surface by oil products," Atmos. Ocean. Phys. **13**, 331–334 (1977).
20. S. Babichenko, A. Dudelzak, and L. Poryvkina, "Laser remote sensing of coastal and terrestrial pollution by FLS-LIDAR," EARSeL eProc. **3**, 1–7 (2004).
21. H. Barth, R. Reuter, and M. Schröder, "Measurement and simulation of substance specific contributions of phytoplankton, gelbstoff, and mineral particles to the underwater light field in coastal waters," EARSeL eProc. **1**, 165–174 (2000).
22. A. M. Chekalyuk, A. A. Demidov, V. V. Fadeev, et al., "Lidar monitoring of phytoplankton and organic matter in the inner seas of Europe," EARSeL Adv. Remote Sens. **3** (3-VII), 131–139 (1995).
23. A. B. Demidov, S. A. Mosharov, V. I. Gagarin, et al., "Spatial variability of the primary production and chlorophyll *a* concentration in the Drake Passage in the Austral Spring," Oceanology (Engl. Transl.) **51**, 281–294 (2011).
24. K. L. Denman and J. F. Dower, "Patch dynamics," in *Encyclopedia of Ocean Sciences* (Academic, London, 2001), pp. 2107–2114.
25. A. E. Detmer and U. V. Bathmann, "Distribution patterns of autotrophic pica- and nanoplankton and their relative contribution to algal biomass during spring in the Atlantic sector of the Southern Ocean," Deep Sea Res., Part II **44** (1–2), 299–320 (1997).
26. C. Eckart, "An analysis of the stirring and mixing processes in incompressible fluids," J. Mar. Res. **7**, 265–275 (1948).
27. S. M. Gallager, C. S. Davis, A. W. Epstein, et al., "High-resolution observations of plankton spatial distributions correlated with hydrography in the Great South Channel, Georges Bank," Deep Sea Res., Part II **43**, 1627–1664 (1996).
28. E. W. Helbling, V. E. Villafane, and O. Holm-Hansen, "Variability of phytoplankton distribution and primary production around Elephant Island, Antarctica, during 1990–1993," Polar Biol. **15**, 233–246 (1995).
29. O. Holm-Hansen and B. Riemann, "Chlorophyll *a* determination: improvements in methodology," Oikos **30**, 438–447 (1978).
30. D. N. Klyshko and V. V. Fadeev, "Remote determination of the admixture concentrations in water by the method of laser spectroscopy using Raman scattering as an internal standard," Sov. Phys. Dokl. **23**, 55–57 (1978).
31. K. Leblanc, B. Quguiner, M. Fiala, et al. "Particulate biogenic silica and carbon production rates and particulate matter distribution in the Indian sector of the subantarctic ocean," Deep Sea Res., Part II **49** (16), 3189–3206 (2002).
32. I. A. Nemirovskaya, "Variability of concentration and composition of hydrocarbons in frontal zones of the Kara Sea," Oceanology (Engl. Transl.) **55**, 497–507 (2015).
33. K. Niewiadomska, H. Claustre, L. Prieur, et al., "Submesoscale physical-biogeochemical coupling across the Ligurian current (northwestern Mediterranean) using a bio-optical glider," Limnol. Oceanogr. **53**, (2008). doi 10.4319/lo.2008.53.5_part_2.2210
34. S. C. Palmer, V. V. Pelevin, I. V. Goncharenko, et al., "Ultraviolet fluorescence LiDAR (UFL) as a measurement tool for water quality parameters in turbid lake conditions," Remote Sens. **5**, 4405–4422 (2013). http://www.mdpi.com/2072-4292/5/9/4405.
35. V. Pelevin, P. Zavialov, B. Konovalov, et al., "Measurements with high spatial resolution of chlorophyll-a, CDOM and total suspended matter in coastal zones and inland water bodies by the portable UFL lidar," *35th EARSeL Symposium "European Remote Sensing: Progress, Challenges and Opportunities"* (Stockholm, 2015). http://www.earsel.org/symposia/2015-symposium-Stockholm/pdf/proceedings/Pelevin.pdf.
36. P. D. Thorne and D. M. Hanes, "A review of acoustic measurement of small-scale sediment processes," Cont. Shelf Res. **22** (4), 603–632 (2002).
37. J. M. G. Vilar, R. V. Sole, and J. M. Rubi, "On the origin of plankton patchiness," Phys. A (Amsterdam, Neth.) **317**, 239–246 (2003).

Translated by G. Karabashev